J Electroceram (2007) 19:311–314
DOI 10.1007/s10832-007-9037-2

# Chemically derived seeding layer for {100}-textured PZT thin films

**F. Tyholdt · F. Calame · K. Prume ·
H. Ræder · P. Muralt**

Received: 20 March 2006 / Accepted: 5 January 2007 /

**Abstract** PZT thin films are used extensively in micro electromechanical systems (MEMS) due to its high piezoelectric coefficients. The electromechanical responses can be optimized by using textured films where the transverse coefficient $e_{31,f}$ is of particular importance for MEMS structures such as cantilevers, bridges and membranes. It has been shown that {100}-textured PZT of morphotropic composition fabricated by chemical solution deposition (CSD) provides the highest transverse coefficient [1]. This specific texture can be obtained using a seeding layer of sputter deposited $PbTiO_3$ [2]. However, in a CSD process it is advantageous to also be able to produce the seed layer by chemical methods. The piezoelectric and dielectric properties of 2 μm PZT film seeded by CSD $PbTiO_3$ measured by a new 4-point bending setup are presented.

**Keywords** PZT · Thin film · Seeding · Chemical solution deposition

## 1 Introduction

Piezoelectric PZT ($Pb(Zr_xTi_{1-x})O_3$) is the most important class of materials for integration in MEMS (Micro Electro-Mechanical System). Their ability to provide electromechanical coupling render this material class very versatile as the active material in actuators, sensors, filters and ultrasonic devices.

It is not possible to grow PZT directly on silicon because of interfacial reactions and Pb–Si interdiffusion at elevated temperatures [3]. Platinum has been demonstrated as a versatile electrode material for ferroelectric materials in general [4–9]. The development of [111] texture for a perovskite as PZT on Pt(111) is expected. The perovskite, with its $ABO_3$ formula (A=Pb and B=Zr/Ti in PZT), in which $AO_3$ forms a face-centered cubic sublattice. In the case of PZT, the (111) planes of the $AO_3$ units and Pt are reasonably well-matched, both having a hexagonal pattern with an interatomic spacing around 2.77 Å. Thus, one should initially expect, since Pt can be grown with a high degree of (111)-texture [10, 11], that one could obtain PZT (111) quite easily using this metal as a substrate. However, high leakage currents have been observed due to low nucleation densities when PZT is growth directly on Pt [10]. It has been demonstrated that both (111) and {100}-texture can be obtained on Pt(111) dependent on processing parameters [5, 12–14]. Especially, the temperature treatment procedure has been found to have a large effect on both formation of the desired perovskite phase, texture and surface morphology. The morphology and the orientation of the PZT crystallites have been shown to have a major effect on the piezoelectric effect of the resulting film. For microsystems where basic structures such as cantilevers, bridges and membranes are typically utilized the transversal coefficient $e_{31,f}$ is of particular importance. The highest

F. Tyholdt (✉) · H. Ræder
SINTEF,
P. O.Box 124 Blindern, 0314 Oslo, Norway
e-mail: frode.tyholdt@sintef.no

F. Calame · P. Muralt
EPFL-LC, MXD Ecublens,
CH-1015 Lausanne, Switzerland

K. Prume
aixACCT Systems GmbH,
Dennewartstr. 25-27,
52068 Aachen, Germany

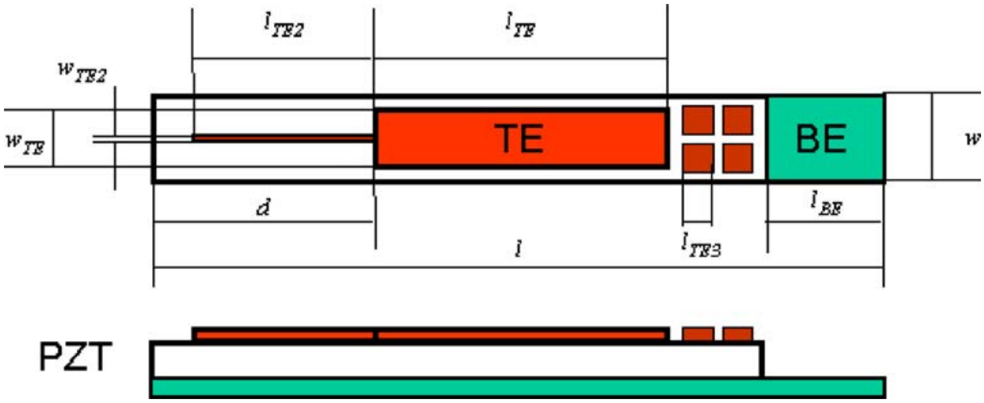

**Fig. 1** Four-point bending sample (© AixACCT Systems GmbH). l=25 mm

transversal piezoelectric coefficient is found in rhombohedral {100} oriented films with a composition close to the morphotropic phase boundary [1, 15–17]. It has been shown that a sputter deposited seed layer of $PbTiO_3$ facilitates fabrication of PZT films with >95% {100} orientation [2] providing a transversal piezoelectric coefficient, $e_{31,f}$, of ~−12 C/m$^2$. In addition, PZT thin films deposited by chemical solution deposition (CSD) exhibits the best electromechanical properties compared to films fabricated with other deposition techniques.

We have developed a qualified procedure for integrating PZT thin films in microsystems on a semi-industrial scale using CSD. To simplify the deposition process it is desirable to also deposit the previously sputter deposited seed layer by CSD. A procedure for seeding {100}-orientation in morphotrophic PZT by CSD has been developed. The dielectric and piezoelectric properties of a 2 μm PZT thin film fabricated using CSD seeding are presented. The transversal piezoelectric coefficient was measured by a new 4-point bending setup that provides a standardized method for measuring this important parameter [18].

## 2 Experimental

A PZT precursor of morphotropic composition, $x$=0.53, was made according to the modified 2-methoxyethanol route described by Gurkovich and Blum [19] and Budd et al. [20] For seeding a similar 0.11 M precursor corresponding to $PbTiO_3$ was made with 30% Pb excess to enhance seed layer orientation and to avoid problems related to lead evaporation. The CSD seed layer was deposited on a platinized silicon wafer (Pt/$TiO_2$/$SiO_2$/Si) using spin coating at 3,000 rpm for 40 s. The film was subsequently pyrolyzed at 350°C for 60 s to evaporate the solvent and pyrolyze the organics after which the seed layer was crystallized at 650°C for 60 s. A 2 μm PZT film was deposited on the seeded wafer using a procedure already described in literature [1]. For measurement of the transversal piezoelectric coefficient using the 4-point bending setup a standardized test sample was fabricated. Such a sample can either be made separately or integrated on a wafer with existing structures for monitoring and quality assurance. Hence, after final crystallization of the

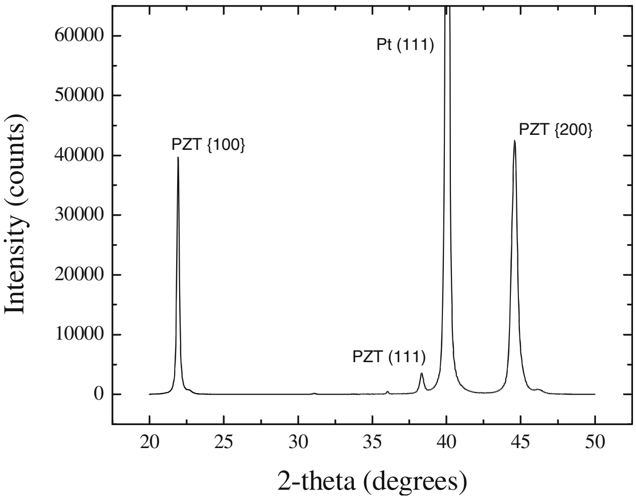

**Fig. 2** X-ray diffractogram of a 2 μm PZT film seeded by CSD $PbTiO_3$

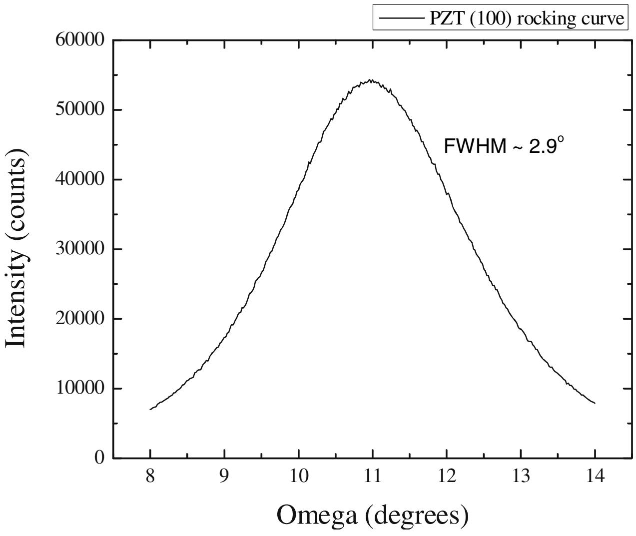

**Fig. 3** Rocking curve of the PZT{100} reflection

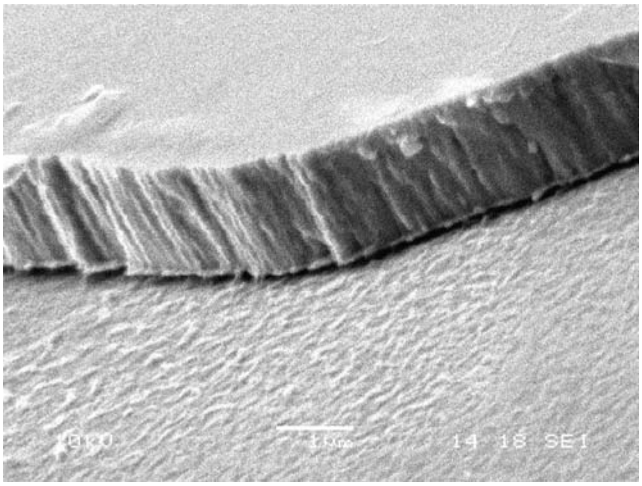

**Fig. 4** SEM picture of a fractured PZT film

film Cr/Au 15/400 nm top electrodes were deposited using thermal evaporation and patterned using lift-off according to the electrode pattern shown in Fig. 1. Contact points to the bottom electrode were fabricated by wet etching of the PZT film [21]. Before measurements the film was poled at 150°C at 200 kV/cm for 10 min. The film was analyzed by X-ray diffraction (Siemens D5000 using $Cu_{K\alpha}$ radiation), scanning electron microscopy (SEM) (JEOL JSM-5400 LV) and scanning transmission electron microscopy (STEM) (FEI Tecnai $G^2$ TF 20 X-Twin) after extraction of a TEM lamellae using focussed ion beam (FIB) (NOVA 600).

## 3 Results and discussion

The X-ray diffractogram in Fig. 2 shows that the film is single phase PZT where the majority of the reflections come from the {100} and {200} planes. The texture (or relative intensities) of the {100} reflection of the film were obtained by normalising the peak intensities of the {100}, (110) and (111) reflections with the corresponding peaks of a randomly oriented powder using the following relation;

$$I^R_{hkl} = \frac{\frac{I_{hkl}}{I^*_{hkl}}}{\sum_{i=1}^{N} \frac{I_{h_ik_il_i}}{I^*_{h_ik_il_i}}}$$

where N is the number of peaks considered (in our case $N$=3) and $I_{hkl}$ and $I^*_{hkl}$ are the integrated XRD peak intensities of the films and the randomly oriented powder of same composition, respectively. A relative orientation of 92% was found. The high orientation is also supported by rocking curve analysis of the {100} reflection in Fig. 2. A full width at half maximum of 2.9° is found (Fig. 3).

Investigation of a fractured film reveals a columnar grain structure which in turn is an indication of heterogeneous nucleation at the seed layer. The bright field TEM image of a cross-section in Fig. 5 show a very dense film with few defects and a thickness close to the targeted 2 µm. The interfaces between the 8 RTP cycles necessary for a film of this thickness can be seen. However, the bright field TEM image in Fig. 5 show that the grains are extending throughout the thickness of the film which indicates that each PZT layer nucleates quasi epitaxially on the previous one. The columnar grains are also clearly seen in intergranular fractures in the film in Fig. 4. The high density of the films can explain the high breakdown strength of these films. The dielectric properties and the transversal piezoelectric coefficient were measured on a 4-point bending sample that was diced out from a full wafer. The film displays a high dielectric coefficient and low loss for a film of this composition and orientation, as can be seen in Table 1. A very high transversal piezoelectric coefficient, $e_{31,f}$, of −14 to −15 C/m$^2$, is measured by the new 4-point bending setup, depending on the mechanical bending excitation frequency (Table 1). The generally accepted value for $e_{31,f}$ until now has been ~−12 C/m$^2$ [22]. We suggest that the high value of the dielectric

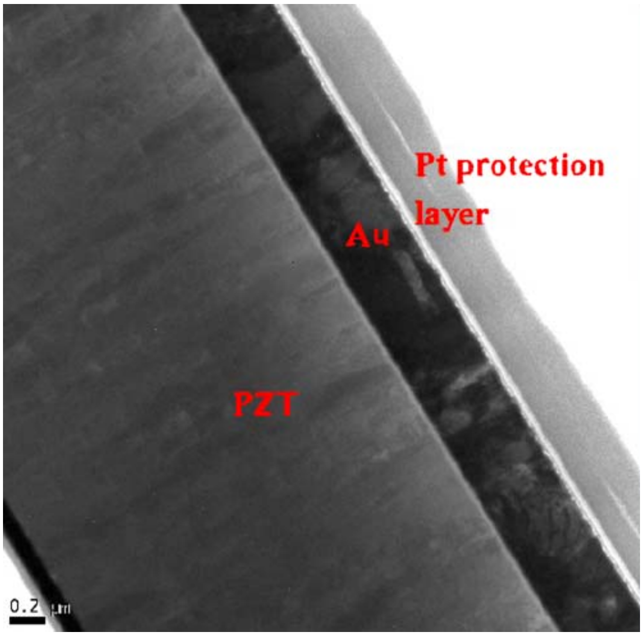

**Fig. 5** TEM picture of a wafer cross-section fabricated by FIB (courtesy of FEI Company ®)

**Table 1** Transversal piezoelectric coefficient and dielectric properties of the 2 µm PZT film.

| Frequency [Hz] | $\varepsilon_{31,f}$ [C/m$^2$] | Relative permittivity, $\varepsilon_r$ | Dissipation factor, tan $\delta$ |
|---|---|---|---|
| 0.1 | −15.1 | | |
| 1 | −14.4 | | |
| 10 | −14.1 | | |
| 1000 | | 1,130 | 0.029 |

constant and $e_{31,f}$ can be attributed to the high orientation and microstructural quality of these films since these parameters generally decreases drastically with decreasing film density. Our experience has been that the use of CSD seeding technique described influences the transversal piezoelectric coefficient favourably compared previously sputtered seed layers.

## 4 Conclusions

High quality thin films of {100}-textured PZT were fabricated using a $PbTiO_3$ seed layer deposited by CSD. The transverse piezoelectric coefficient, $e_{31,f}$, was found to be −15.1 C/m$^2$ as measured by a new 4-point bending setup by aixACCT systems. The described process yielded dense and crack-free films, with high breakdown strength, that facilitated poling at 200 kV/cm. The excellent dielectric and piezoelectric properties of the resulting PZT film and the simplicity of the procedure makes the developed seeding procedure preferred for integration of PZT in MEMS.

**Acknowledgements** This work has been a part of the MEMS-pie cooperative research project which is funded by the 6th framework program of the European Commission (Contract no. COOP-CT-2004-508219)

## References

1. N. Ledermann, P. Muralt, J. Baborowski, S. Gentil, K. Mukati, M. Cantoni, A. Seifert, N. Setter, Sens. Actuators, A, Phys. **A105**, 162 (2003)
2. T. Maeder, P. Muralt, M. Kohli, A. Kholkin, N. Setter, Br. Ceram. Proc. **54**, 207 (1995)
3. P. Revesz, J. Li, N. Szabo Jr., J.W. Mayer, D. Caudillo, E.R. Myers, Mater. Res. Soc. Symp. Proc. **243**, 101 (1992)
4. J. Chen, K.R. Udayakumar, K.G. Brooks, L.E. Cross, J. Appl. Phys. **71**, 4465 (1992)
5. K.G. Brooks, I.M. Reaney, R. Klissurska, Y. Huang, L. Bursill, N. Setter, J. Mater. Res. **9**, 2540 (1994)
6. H.N. Al-Shareef, K.D. Gifford, S.H. Rou, P.D. Hren, O. Auciello, A.I. Kingon, Integr. Ferroelectr. **3**, 321 (1993)
7. K.D. Budd, D.A. Payne, Inst. Phys. Conf. Ser. 13 (1989)
8. T. Nasu, M. Kibe, Y. Uemoto, E. Fujii, T. Otsuki, Jpn. J. Appl. Phys., Part 1 (Regular Papers, Short Notes and Review Papers) **37**, 4144 (1998)
9. T. Maeder, L. Sagalowicz, P. Muralt, Jpn. J. Appl. Phys., Part 1 (Regular Papers, Short Notes and Review Papers) **37**, 2007 (1998)
10. K. Aoki, Y. Fukuda, K. Numata, A. Nishimura, Jpn. J. Appl. Phys., Part 1 (Regular Papers, Short Notes and Review Papers) **34**, 192 (1995)
11. P. Muralt, T. Maeder, L. Sagalowicz, S. Hiboux, S. Scalese, D. Naumovic, R.G. Agostino, N. Xanthopoulos, H.J. Mathieu, L. Patthey, E.L. Bullock, J. Appl. Phys. **83**, 3835 (1998)
12. L.A. Bursill, I.M. Reaney, D.P. Vijay, S.B. Desu, J. Appl. Phys. **75**, 1521 (1994)
13. S.Y. Chen, I.W Chen, J. Am. Ceram. Soc. **77**, 2332 (1994)
14. S.Y. Chen, I.W. Chen, J. Am. Ceram. Soc. **77**, 2337 (1994)
15. A. Seifert, N. Ledermann, S. Hiboux, J. Baborowski, P. Muralt, N. Setter, Integr. Ferroelectr. **35**, 159 (2001)
16. M.A. Dubois, P. Muralt, D.V. Taylor, S. Hiboux, Integr. Ferroelectr. **22**, 1055 (1998)
17. D.V. Taylor, D. Damjanovic, Appl. Phys. Lett.**76**, 1615 (2000)
18. K. Prume, P. Muralt, F. Calame, T. Schmitz-Kempen, S. Tiedke, IEEE Trans. Ultrason. Ferroelectr. Freq. Control **54**, 8 (2007)
19. S.R. Gurkovich, J.B. Blum, in *Preparation of Monolithic Lead Titanate by A Sol-gel Process* (Wiley, NY, 1984), p. 152
20. K.D. Budd, S.K. Dey, D.A. Payne, Br. Ceram. Proc. **36**, 107 (1985)
21. L.P. Wang, R. Wolf, Q. Zhou, S. Trolier-McKinstry, R.J. Davis, Mater. Res. Soc. Symp. Proc. **657**, EE5 39/1 (2001)
22. S. Trolier-McKinstry, P. Muralt, J. Electroceram. **12**, 7 (2004)